J Mater Sci (2007) 42:5860–5866
DOI 10.1007/s10853-006-1141-1

Preparation and electrical properties of sintered oxides composed of $Mn_{1.5}Co_{(0.25+X)}Ni_{(1.25-X)}O_4$ ($0 \leqq X \leqq 0.75$) with a cubic spinel structure

T. Yokoyama · T. Meguro · Y. Shimada · J. Tatami · K. Komeya · Y. Abe

Received: 17 August 2004 / Accepted: 18 November 2005 / Published online: 24 May 2007

Abstract Monophase cubic spinel-type oxides of $Mn_{1.5}Co_{(0.25+X)}Ni_{(1.25-X)}O_4$ ($0 \leqq X \leqq 1$) were prepared through the oxidation of specimens sintered at 1400 °C. The oxides with $0 \leqq X \leqq 0.75$ composition are focused on in this study, as the oxides with $0.75 < X \leqq 1$ composition did not convert into a monophase cubic spinel structure. The electrical conductivity of the sintered bodies was confirmed to increase exponentially with increasing temperature. In the composition range of $0 \leqq X \leqq 0.75$, both the electrical conductivity and the Seebeck coefficient increased with increasing X. The oxides with composition between $0 \leqq X < 0.57$ were *n*-type semiconductors, whereas those with $0.57 < X \leqq 0.75$ were *p*-type. It was concluded that electrical conduction in the specimens is controlled by small polaron hopping.

Introduction

Complex oxides composed of transition metals such as Mn, Fe, Co, and Ni are widely used as negative temperature coefficient (NTC) thermistors for temperature measurement and control. In recent years, there has been extensive research regarding these materials for the purposes of producing cheap, high quality thermistors [1–8].

Our laboratory has focused on preparation methods specific to the Mn–Co–Ni ternary oxide system and their electrical properties [1, 2, 4, 7–11]. In particular, the specific composition of the ternary system that allows for the practical preparation of sintered bodies with a monophase cubic spinel structure is of particular interest because of the electrical conduction properties associated with this structure. The principle in manufacturing sintered bodies with a monophase cubic spinel structure is to oxidize the initial oxides, which are sintered at 1400 °C in an inert gas. This oxidation must be conducted in air at temperatures below 1000 °C, where the cubic spinel phase is stable. The stable phase of the ternary system was previously examined at temperatures from 700 to 1100 °C to establish the composition range of the monophase cubic spinel-type crystals [12]. Using the phase diagram of 800 °C, the authors have investigated the manufacturing of monophase sintered bodies. The region of cubic spinel-type monophase is enclosed with points of Mn:Co = 1.25:1.75, Mn:Co = 0:1, Mn:Ni = 2:1, and Mn:Ni = 1.75:1.25, as is shown in Fig. 1.

So for the sintered bodies composed of $Mn_{(2-X)}Co_{2X}Ni_{(1-X)}O_4$ ($0 \leqq X \leqq 1$) [2], $Mn_{(1.5-0.5X)}Co_{(1+0.5X)}Ni_{0.5}O_4$ ($0 \leqq X \leqq 1$) [4, 7], and $Mn_{(1.5-0.25X)}CoNi_{(0.5+0.25X)}O_4$ ($0 \leqq X \leqq 1$) [8] were fabricated and their respective electrical properties were examined. These lines are included in Fig. 1. A series of studies suggested that the composition dependence of the electrical properties was based on the ratio of Mn^{3+} to Mn^{4+} ions in the octahedral sites of the spinel structure, and that the electrical conduction of the oxides was

T. Yokoyama (✉) · T. Meguro · Y. Shimada · J. Tatami · K. Komeya
Yokohama National University, 79-5 Tokiwadai, Hodogaya-ku, Yokohama-shi 240-8501, Japan
e-mail: t-yoko@ynu.ac.jp

Y. Abe
Technol Seven Co. Ltd., 25-6 Tobehonmachi, Nishi-ku, Yokohama-shi 226-0041, Japan

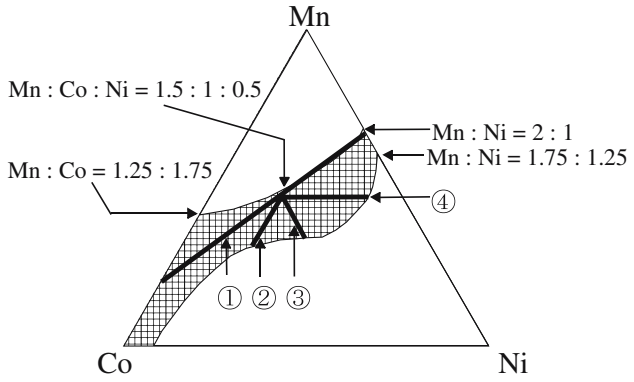

Fig. 1 Phase relation in Mn–Co–Ni oxides fired at 800 °C for 3 h. ■: Cubic spinel monophase region, ①: $Mn_{(2-X)}Co_{2X}Ni_{(1-X)}O4$ ($0 \leqq X \leqq 1$) [2], ②: $Mn_{(1.5-0.5X)}Co_{(1+0.5X)}Ni_{0.5}O_4$ ($0 \leqq X \leqq 1$) [4, 7], ③: $Mn_{(1.5-0.25X)}CoNi_{(0.5+0.25X)}O_4$ ($0 \leqq X \leqq 1$) [8], ④: $Mn_{1.5}Co_{(0.25+X)}Ni_{(1.25-X)}O_4$ ($0 \leqq X \leqq 1$) (This study)

controlled by a small polaron hopping mechanism. In the studies on the $Mn_{(1.5-0.5X)}Co_{(1+0.5X)}Ni_{0.5}O_4$ [4, 7] and $Mn_{(1.5-0.25X)}CoNi_{(0.5+0.25X)}O_4$ [8] systems, the electrical conductivity (σ) was found to decrease with increasing X. The current goal of our research is to map semiconductor properties such as electrical conduction, carrier concentration, mobility, activation energy, the Seebeck coefficient, and so on. These maps will be of assistance in designing new thermistor materials corresponding to various needs.

This paper is a part of this investigative program and focuses on the oxides located on line ④ in Fig. 1 expressed as $Mn_{1.5}Co_{(0.25+X)}Ni_{(1.25-X)}O_4$ ($0 \leqq X \leqq 1$).

Experimental

Starting materials with the compositions shown in Table 1 were prepared by mixing Mn, Co, and Ni nitrates followed by evaporating to dryness. The mixtures were molded into disks 25 mm in diameter and 5 mm thick. To prepare sintered bodies with monophase cubic spinel structures, these pellets were heated from room temperature to 1000 °C over 1 h, further heated to 1400 °C over 1 h, and then held at this temperature to sinter for 3 h, all in an argon atmosphere. The sintered specimens were then cooled to 800 °C, and then exposed to air to oxidize the rock salt-type oxides. The phases present in the specimens oxidized at 800 °C for 0, 0.5, 1, 3, 48, and 144 h were analyzed by X-ray diffraction after quenching in water.

σ and the Seebeck potential (Qe) were measured in argon using a rectangular specimen ($3 \times 3 \times 15$ mm) cut from a sintered pellet consisting of monophase cubic spinel-type oxides. σ was determined by the DC four-probe method at temperatures ranging from 100 to 300 °C. Qe was measured with a difference of around 5 °C between the ends of the rectangular specimen at temperatures from 100 to 300 °C.

Table 1 Compositions of specimens

X	Mn:Co:Ni
0.00	1.50:0.25:1.25
0.22	1.50:0.47:1.03
0.25	1.50:0.50:1.00
0.28	1.50:0.53:0.97
0.50	1.50:0.75:0.75
0.54	1.50:0.79:0.71
0.57	1.50:0.82:0.68
0.60	1.50:0.85:0.65
0.72	1.50:0.97:0.53
0.75	1.50:1.00:0.50
1.00	1.50:1.25:0.25

Results and discussion

Preparation of monophase cubic spinel oxides

Figures 2a and b show the X-ray diffraction patterns of specimens with $X = 0.75$ and $X = 1$, which were both oxidized at 800 °C for 48 and 144 h. In the $X = 0.75$ specimen, the 48 h oxidation profile indicated a monophase cubic spinel-type structure, as shown in Fig. 2a. Other specimens with between $X = 0$ and 0.72 were also confirmed to have perfectly converted into cubic spinel structure during the 48 h oxidation.

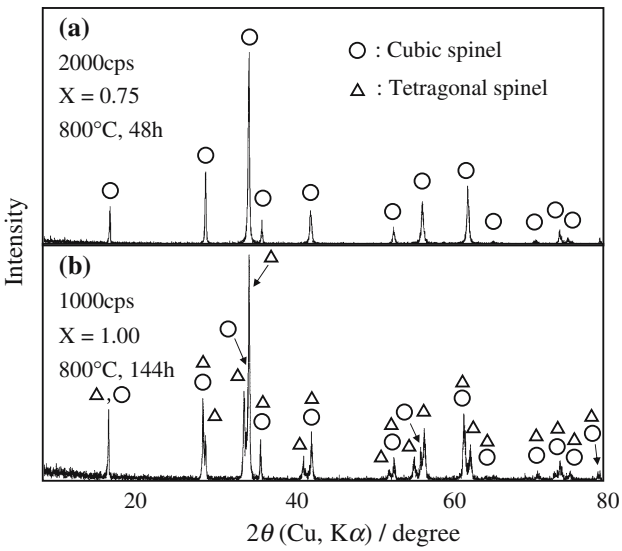

Fig. 2 X-ray diffraction patterns of specimens with $X = 0.75$ and $X = 1$ which were oxidized at 800 °C after firing at 1400 °C. (**a**) $X = 0.75$, (**b**) $X = 1$

However, the profile of the specimen with $X = 1$ showed peaks based on a tetragonal spinel structure in addition to a cubic spinel structure. The extension of the heating from 48 h to 144 h had no effect on the tetragonal spinel peaks, as is clear in Fig. 2b. Although Fig. 1 shows that the composition of $X = 1$ is in cubic spinel region, the sintered specimen is out of the monophase. The reason for this difference may be due to the difference in heating history. The experiment was performed under condition that starting oxides obtained by the thermal decomposition of starting materials were heated directly to 800 °C and then quenched after 3 h through soaking. Thus the specimen with $X = 1$ was omitted in this experiments without follow-up research. Since the sintered bodies had more or less cracks when they were quenched into water, the specimens gradually cooled to room temperature after oxidizing at 800 °C for oxidation were used for measurements of lattice constants and electrical properties. These specimens were confirmed to have monophase cubic spinel structure as well as those specimens quenched into water.

Figure 3 illustrates the change in the lattice constant as a function of X. In the region $0 \leqq X \leqq 0.25$, the lattice constant decreases with increasing X. In the region $0.25 \leqq X \leqq 0.75$, it increases gradually with increasing X. The slope changes at the point $X = 0.25$, indicating a transformation of the substitution mode in the cation distribution. The cation distribution of $Mn_{1.5}CoNi_{0.5}O_4$ ($X = 0.75$) was estimated using Eq. 1 in our previous paper [2].

$$(Co^{2+}_{0.58}Mn^{2+}_{0.42})[Ni^{2+}_{0.5}Co^{3+}_{0.42}Mn^{3+}_{0.58}Mn^{4+}_{0.5}]O^{2-}_4 \quad (1)$$

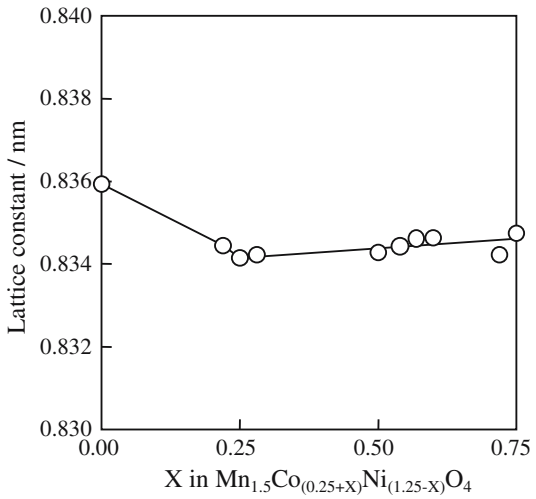

Fig. 3 Lattice constants as a function of X in $Mn_{1.5}Co_{(0.25+X)}Ni_{(1.25-X)}O_4$

Here, ( ) represents a tetrahedral site, and [ ] an octahedral site. Equation 1 shows that Mn^{2+} and Co^{2+} occupy the tetrahedral sites and that Ni^{2+}, Mn^{4+}, Mn^{3+}, and Co^{3+} occupy the octahedral sites. However, the distribution of the compositions, with the exception of $X = 0.75$, are not yet understood. Therefore, we cannot discuss at present the relationship between the change in lattice constant and the substitution mode.

Composition dependence of electrical conductivity and Seebeck coefficient

Figure 4 shows the relationship between σ and temperature. σ increases exponentially with increasing temperature, which indicates that these oxides have intrinsic NTC thermistor characteristics. Figure 5 is a plot of σ as a function of X, which clearly shows that σ increases with increasing X.

To investigate the composition dependence of σ, the B values, which are used to evaluate the characteristics of a thermistor, were calculated from the results of σ using Eq. 2:

$$\sigma_2 = \sigma_1 \exp\{(1/T_1 - 1/T_2)\} \quad (2)$$

Here, σ_1 and σ_2 are σ values at temperatures of T_1 and T_2, respectively, and B is called the thermistor constant (apparent activation energy of σ) [13, 14]. In this calculation, T_1 and T_2 were selected as 473.15 K and 573.15 K. Figure 6 demonstrates the composition dependence of the B value. It is found that the B

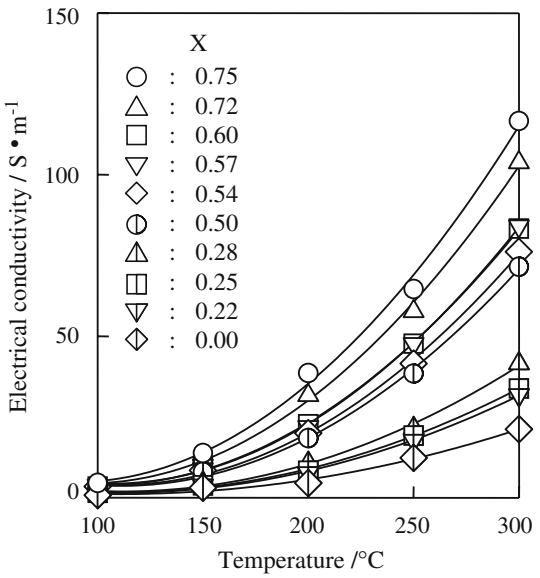

Fig. 4 Temperature dependence of electrical conductivity of specimens with various compositions

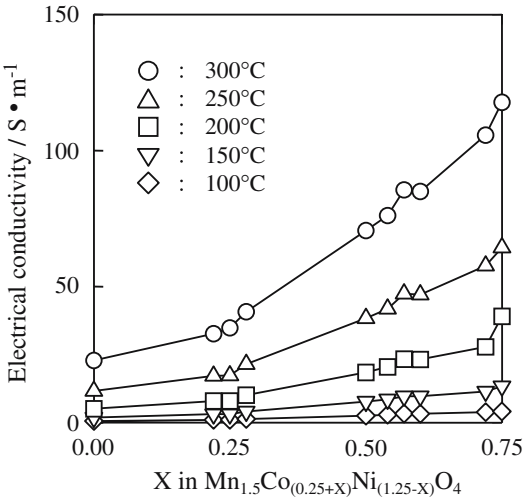

Fig. 5 Electrical conductivity as a function of X in $Mn_{1.5}Co_{(0.25+X)}Ni_{(1.25-X)}O_4$

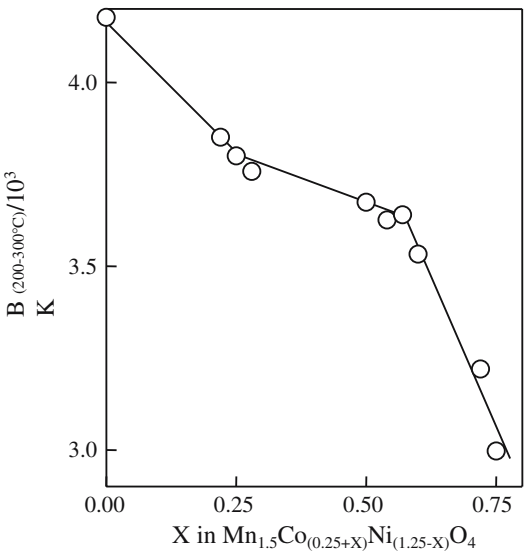

Fig. 6 Changes in thermistor constant, B value, as a function of X in $Mn_{1.5}Co_{(0.25+X)}Ni_{(1.25-X)}O_4$

value decreases with increasing X, as shown by the three straight lines with two turning points at $X = 0.25$ and 0.57. These turning points will be discussed later.

Figure 7 demonstrates the composition dependence of the Seebeck coefficient (Qs) of each sintered body, which was estimated at various temperatures. Qs is recognized to be independent of temperature, and increases with increasing X in the region $0.25 \leqq X \leqq 0.75$, whereas the composition dependence is small in the region $0 \leqq X \leqq 0.25$. The composition at $X = 0.25$ agrees well with the composition at the

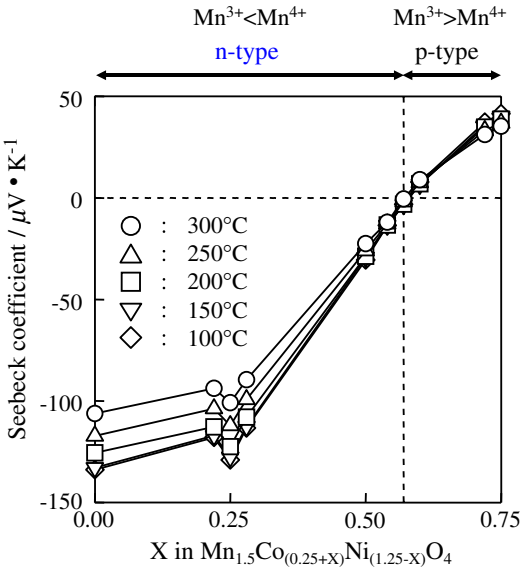

Fig. 7 Seebeck coefficient as a function of X in $Mn_{1.5}Co_{(0.25+X)}Ni_{(1.25-X)}O_4$ at various temperatures

turning point shown in Fig. 3 and Fig. 6. The change at $X = 0.25$ is related to the substitution mode of cations in the octahedral sites. The specimens in the region of $0 \leqq X \leqq 0.57$ are considered to be n-type semiconductors based on negative Qs values, compared with positive Qs p-type semiconductors in other regions.

It was concluded in a previous paper [2] that the electrical conduction of $Mn_{1.5}CoNi_{0.5}O_4$ ($X = 0.75$) is due to small polaron hopping. The cation distribution in Eq. 1 shows that hopping occurs between Mn^{3+} and Mn^{4+} [2, 15], assuming the valence numbers of the other cations in the octahedral sites such as Ni^{2+} and Co^{3+} are fixed [2]. The cation distributions of other specimens were not estimated. However, it is speculated that the conduction of these other specimens is the same as that of the specimen with $X = 0.75$. In the region $0 \leqq X < 0.57$, Qs is negative, indicating that the carriers in the oxides are electrons, as the amount of Mn^{3+} is less than that of Mn^{4+} in the octahedral sites. In the region $0.57 < X \leqq 0.75$, Qs is positive, indicating that the carriers of the oxides are holes because Mn^{3+} is larger than Mn^{4+} in the octahedral sites. The composition at $X = 0.57$ agrees well with the composition at the turning point shown in Fig. 6. A change in the substitution mode can be ruled out because the change in the lattice constant is continuous in the region $0.25 \leqq X \leqq 0.75$. The turning point at $X = 0.57$ seen in Fig. 6 is thought to correspond to the carrier Mn^{3+} changing to Mn^{4+}.

Composition dependence of carrier concentration and mobility

The carrier concentration (n) can be calculated using Eqs. 3 and 4.

$$|Qs| = (k/e)\{\ln(Nv/n) + \alpha\} \quad (3)$$

$$Nv = 16/a^3 \quad (4)$$

Here, k is Boltzmann's constant, e is the electric charge, Nv is the density of states in the valence band, α is a constant depending on the dominant scattering mechanism (α was neglected for this calculation), a is the lattice constant, and 16 is the number of octahedral sites in a unit cell. The composition dependence of n measured at various temperatures is shown in Fig. 8. n seems to be independent of temperature, indicating that the electrical conduction is due to small polaron hopping. n appears to be almost constant in the region $0 \leqq X \leqq 0.25$, and increases rapidly with increasing X in the region $0.25 \leqq X \leqq 0.57$. In the region $0.57 \leqq X \leqq 0.75$, n decreases suddenly with increasing X. The point at $X = 0.57$ is the maximum in the specimens, which implies that the ratio Mn^{3+}/Mn^{4+} is near unity.

The mobility (μ) was calculated from Eq. 5.

$$\sigma = ne\mu \quad (5)$$

Figure 9 illustrates the temperature dependence of μ. It increases exponentially with increasing temperature. The composition dependence of μ was examined base on the data in Fig. 9. As shown in Fig. 10, μ of the specimen with $X = 0.25$ is slightly higher compared with $X = 0$, decreases in the direction of $X = 0.57$, and increases with increasing X beyond $X = 0.57$.

To investigate the composition dependence of σ shown in Fig. 5, the relationship between n and μ at 300 °C was plotted. The results are shown in Fig. 11. Comparing Fig. 5 with Fig. 11 reveals that the increase in σ is small, as the values of n and μ of specimens in the range $0 \leqq X \leqq 0.25$ are also small. In the region $0.25 \leqq X \leqq 0.57$, σ increases with increasing n under the

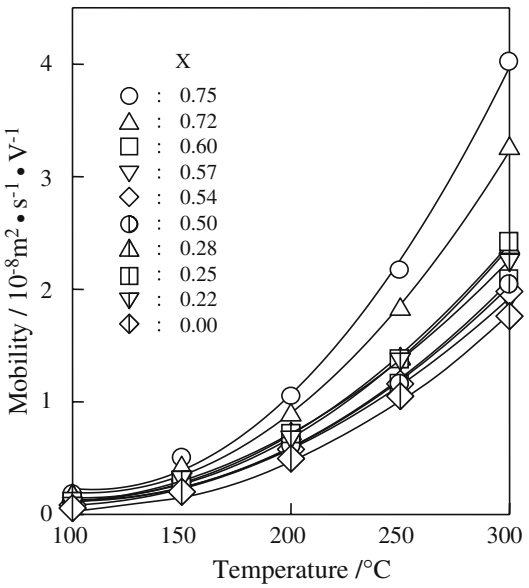

Fig. 9 Temperature dependence of mobility of specimens

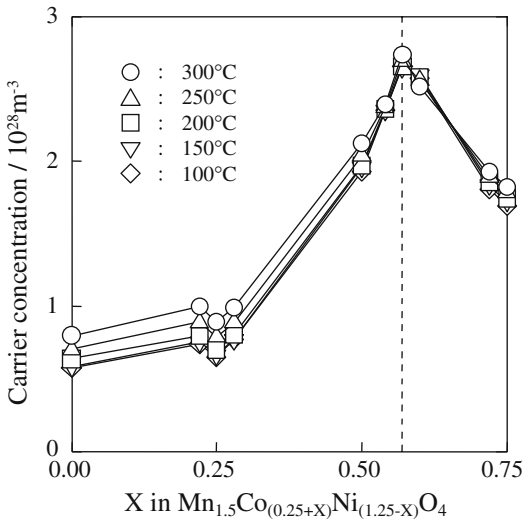

Fig. 8 Carrier concentration as a function of X in $Mn_{1.5}Co_{(0.25+X)}Ni_{(1.25-X)}O_4$

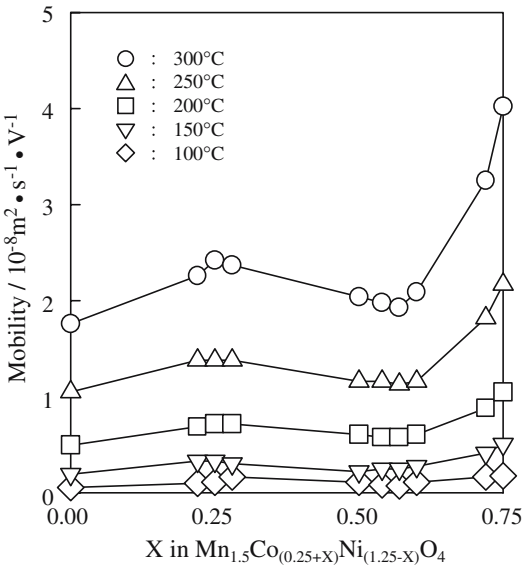

Fig. 10 Mobility as a function of X in $Mn_{1.5}Co_{(0.25+X)}Ni_{(1.25-X)}O_4$

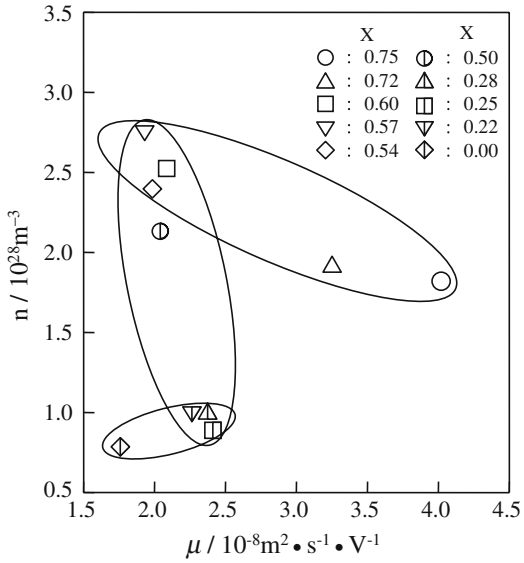

Fig. 11 Relationship between carrier concentration and mobility evaluated at 300 °C

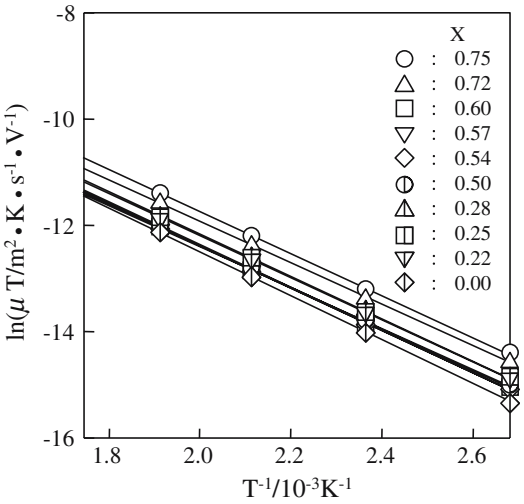

Fig. 12 Plots of $\ln(\mu T)$ as a function of reciprocal T

condition where almost no change of μ occurs. In the region $0.57 \leqq X \leqq 0.75$, σ increases with increasing μ.

In general, it is known that the conduction is due to a small polaron hopping mechanism in the case where μ, having less than $10^{-6}\,m^2\,s^{-1}\,V^{-1}$, tends to increase with increasing temperature [16–21]. Given that the specimens fabricated in this study also satisfy these conditions, it is concluded that the electrical conduction observed in this study is the result of this hopping mechanism as well.

The relationship between μ and the absolute temperature (T) was examined to investigate the conduction mechanism in $Mn_{1.5}Co_{(0.25+X)}Ni_{(1.25-X)}O_4$ ($0 \leqq X \leqq 0.75$). Generally, it is expressed by Eq. 6 [16].

$$\mu T = (ed^2 v_0/K)\exp(-E\mu/kT) \tag{6}$$

Here, d is the jump distance for charge carriers, v_o is the charge carrier jump frequency, and $E\mu$ is the activation energy of μ. Equation 6 indicates that the plots of logarithmic μT against reciprocal T present a linear relationship with a slope equal to the value of $E\mu$. These plots are shown in Fig. 12. The calculated values of $E\mu$ were found to be in the range from 0.33 to 0.36 eV. These values support the above argument, as past research has indicated $E\mu$ is in the range of 0.1 to 0.5 eV [22].

To clarify the composition dependence of μ, the relationships between μ with d and v_o as evaluated using Eq. 6 were examined. d^2 values in the specimens with $0 \leqq X \leqq 0.75$ were calculated to be between $8.70 \times 10^{-2}\,nm^2$ and $8.73 \times 10^{-2}\,nm^2$, suggesting that

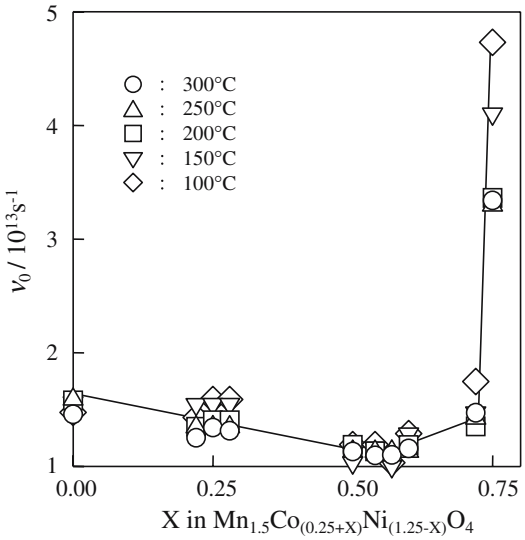

Fig. 13 Charge carrier jump frequency as a function of X in $Mn_{1.5}Co_{(0.25+X)}Ni_{(1.25-X)}O_4$

they are almost constant. Figure 13 illustrates the composition dependence of v_o calculated using Eq. 6. Jonker and Houten discussed on the semiconductor characteristics of several oxides and reported that v_o is in the range from 10^{11} to $10^{13}\,s^{-1}$ [16]. In this study, the values of v_o are found to be in the order of $10^{12}\,s^{-1}$, which is in agreement with their values. In the region $0 \leqq X \leqq 0.57$, v_o decreases gradually with increasing X, and increases rapidly with increasing X in the region $0.57 \leqq X \leqq 0.75$. The composition at $X = 0.57$ is in good agreement with the composition at the turning points seen in Figs. 6, 8, 10, and 11. It is believed that the increase in v_o corresponds to the increase in μ.

The 3d orbitals of Mn^{3+} have four electrons. The three electrons occupy the energy level of t_{2g} and one electron occupies e_g. The 3d orbitals of Mn^{4+} have three electrons, and these electrons occupy only the energy level of t_{2g}. The e_g electron of Mn^{3+} is easy to be excited and more mobile than the t_{2g} electrons of Mn^{4+}. When the concentration of Mn^{3+} in the octahedral sites is high, v_o is expected to be also high. Practically v_o increases above $X = 0.57$, which is compatible to the estimated cation distribution (Eq. 1) implying that the content of Mn^{3+} is higher than that of Mn^{4+} for the composition of $X = 0.75$. Here X is supposed to be expanded to the region of $0.57 < X \leqq 0.75$, because the Qs values are positive. However, the reason why v_o steeply increases toward 0.75 is obscure. To clarify this phenomenon, information of exact cation distributions and further discussion are required.

Conclusion

In this paper, the preparation and electrical properties of sintered bodies consisting of a monophase cubic spinel-type oxide, $Mn_{1.5}Co_{(0.25+X)}Ni_{(1.25-X)}O_4$ ($0 \leqq X \leqq 1$), were investigated. The conclusions of this study can be summarized as follows.

1. In the region $0 \leqq X \leqq 0.75$, the sintered bodies manufactured at 1400 °C were completely converted to monophase cubic spinel-type oxides by heat treatment at 800 °C for 48 h in air. However, the conversion of the oxides with $0.75 < X \leqq 1$ was incomplete even though they were heat-treated for more than 144 h.
2. The electrical conductivity (σ) increased exponentially with increasing temperature, indicating that these oxides have intrinsic NTC thermistor characteristics. σ increased with increasing Co concentration with a constant Mn concentration.
3. The oxides with $0 \leqq X < 0.57$ were *n*-type semiconductors, whereas those with $0.57 < X \leqq 0.75$ were *p*-type. This change is likely associated with the ratio of Mn^{3+} to Mn^{4+} ions in the octahedral sites.
4. The electrical conduction of the oxides is controlled by the small polaron hopping mechanism.

References

1. Yokoyama T, Kondo K, Komeya K, Meguro T, Abe Y, Sasamoto T (1995) J Mater Sci 30:1845
2. Yokoyama T, Abe Y, Meguro T, Komeya K, Kondo K, Kaneko S, Sasamoto T (1996) Jpn J Appl Phys 35:5775
3. Hosseini M (2000) Ceram Intern 26:245
4. Yokoyama T, Meguro T, Morita T, Abe Y, Tatami J, Komeya K, Kumashiro Y (2000) J Aust Ceram Soc 36:133
5. Altenburg H, Mrooz O, Plewa J, Shpotyuk O, Vakiv M (2001) J Eur Ceram Soc 21:1787
6. Park K, Bang DY, Kim JG, Kim JY, Lee CH, Choi BH (2002) J Korean Phys Soc 41:251
7. Abe Y, Meguro T, Yokoyama T, Morita T, Tatami J, Komeya K (2003) J Ceram Process Res 4:140
8. Meguro T, Hisayasu T, Abe Y, Yokoyama T, Komeya K, Tatami J (2004) J Mater Sci Soc Jpn 41:31
9. Meguro T, Sasamoto T, Yokoyama T, Shiraishi T, Abe Y, Torikai N, (1988) J Ceram Soc Jpn 96:338
10. Yokoyama T, Meguro T, Sasamoto T, Yamada S, Abe Y, Torikai N (1988) J Ceram Soc Jpn 96:985
11. Meguro T, Yokoyama T, Komeya K (1992) J Mater Sci 27:5529
12. Abe Y, Meguro T, Oyamatsu S, Yokoyama T, Komeya K (1999) J Mater Sci 34:4639
13. Sinnott MJ (1958) The solid state for engineers. John Wiley & Sons, Inc., New York, p 369
14. Futaki H (1969) S misuta to Sonooyo. Niikankogyosinbunsha, Tokyo, p 3
15. Dannenberg R, Baliga S, Gambino RJ, King AH, Doctor AP (1999) J Appl Phys 86:514
16. Jonker GH, Van Houten S (1961) In: Köhn FS (ed) Halbleiterprobleme. Frieder Vieweg & Sohn, Braunschweing, p 118
17. Mitoff SP (1966) Progr Ceram Sci 4:217
18. Rathenad GW, Goodenough JB (1968) J Appl Phys 39:403
19. Goodenough JB (1971) Progr Solid State Chem 5:145
20. Johannesen ϕ, Kofstad P (1985) J Mater Educ 7:915
21. Moulson AJ, Herbert JM (2003) Electroceramics. John Wiley & Sons Ltd., England, p 5
22. Mizuta S, Koumoto K (1986) In: Douyama M, Yamamoto R (eds) Seramikku zairyo. Tokyo Daigaku Syuppan, Tokyo, p 33